Use of auxiliary data of topography, snow and ice to improve model performance in a glacier-dominated catchment in Central Asia

Hongkai Gao, Tianding Han, Youcun Liu and Qiudong Zhao

ABSTRACT

Whether coupling auxiliary information (except for conventional rainfall–runoff and temperature data) into hydrological models can improve model performance and transferability is still an open question. In this study, we chose a glacier catchment to test the effect of auxiliary information, i.e., distributed forcing input, topography, snow-ice accumulation and melting on model calibration–validation and transferability. First, we applied the point observed precipitation and temperature as forcing data, to test the model performance in calibration–validation and transferability. Second, we took spatial distribution of forcing data into account, and did the same test. Third, the aspect was involved to do an identical experiment. Finally, the snow–ice simulation was used as part of the objective function in calibration, and to conduct the same experiment. Through stepwisely accounting these three pieces of auxiliary information, we found that a model without involving forcing data distribution, local relief, or snow–ice data can also perform well in calibration, but adding forcing data distribution and topography can dramatically increase model validation and transferability. It is also remarkable that including the snow–ice simulation into objective function did not improve model performance and transferability in this study. This may be because the well-gauged hydro-meteorological data are sufficient to constrain a well-designed hydrological model.

Key words | auxiliary information, glacier hydrology, model transferability, Urumqi No.1 Glacier

Hongkai Gao
Julie Ann Wrigley Global Institute of Sustainability,
Arizona State University,
Tempe,
AZ 85287,
USA

Hongkai Gao
Tianding Han (corresponding author)
State Key Laboratory of Cryospheric Sciences, Cold and Arid Regions Environmental and Engineering Research Institute,
Chinese Academy of Sciences,
Lanzhou,
China
E-mail: *tdhan@lzb.ac.cn*

Youcun Liu
Qiudong Zhao
Tianjin Key Laboratory of Water Resources and Environment,
Tianjin Normal University,
No. 393 Binshuixi Road, Xiqing District,
Tianjin,
China

INTRODUCTION

'Auxiliary' data in rainfall–runoff modelling are here defined as all data except conventional meteorological data (i.e., precipitation and temperature) and streamflow data which are indispensable information to force and calibrate hydrological models. The auxiliary data include, but are not limited to, observed evaporation (Baldocchi *et al.* 2001; Xiao *et al.* 2012), isotopic data to separate hydrographs (Uhlenbrook & Hoeg 2003; Weiler *et al.* 2003; Klaus & McDonnell 2013), saturated area fraction (Troch *et al.* 2001), groundwater level (Seibert 2003; Fenicia *et al.* 2008; Li *et al.* 2015a), lake water level (Duan & Bastiaanssen 2013; Lindström 2016), snow and ice depth (Pomeroy *et al.* 2007; Singh *et al.* 2008; Moore *et al.* 2009; Gao *et al.* 2012; Li *et al.* 2015b), and topography (Beven & Kirkby 1979; Gharari *et al.* 2011; Sun *et al.* 2017), etc. Vast amounts of *in situ* and remote sensing data are explosively accumulating and easier to access. Unfortunately, at least in practical implementation, it is still not uncommon that the only input for hydrological models are the conventional meteorological data as forcing, and streamflow data are utilized as an objective to calibrate and validate parameter sets with fixed model structures.

With auxiliary information, whether we can improve model performance or merely increase model redundancy is still an unaddressed question. Some hydrologists have

doi: 10.2166/nh.2016.242

found that auxiliary information was useful to improve model performance, and some drew the opposite conclusion. For example, Winsemius *et al.* (2009) used satellite data, i.e., remote sensed evaporation, as auxiliary information to calibrate a model and gain deeper understanding of the hydrological processes in a real ungauged basin in Africa. Fenicia *et al.* (2008) used groundwater and water isotope auxiliary data in addition to streamflow to understand how different sources of data can motivate model development and help to understand catchment behavior. They found that both groundwater and isotope data could be used to understand threshold processes and mixing processes in the catchment, respectively. Tangdamrongsub *et al.* (2015) found that data assimilation of GRACE terrestrial water storage into a hydrological model had improved groundwater estimation, but not in streamflow estimation. Sometimes, due to observation artifacts, auxiliary data do not have undoubted superiority over simulated results. For example, Winsemius *et al.* (2006) found the discrepancy of GRACE and a hydrological model is probably caused by the data quality of GRACE; Matgen *et al.* (2012) found that assimilating the remote sensing soil moisture even resulted in a negative impact on discharge simulation.

In spite of the availability of auxiliary information, most studies have focused on the impact of model performance in either internal fluxes or streamflow (Hailegeorgis & Alfredsen 2015; Li *et al.* 2015a), and the impact of auxiliary information on model transferability is rarely tested. Therefore, hydrological model transferability is still a great challenge in the hydrology community (Hrachowitz *et al.* 2013; Biondi & De Luca 2017). Beyond calibration–validation for one catchment, model transferability can serve as an indicator to more rigorous testing (Refsgaard *et al.* 2014) of their physical realism, and whether models get the right answer for the right reasons (Kirchner 2006). Model transferability is also related to model upscaling (Hrachowitz *et al.* 2013; Gao *et al.* 2014a), which is essential in hydrological modeling and water resources management. Ignoring catchment landscape heterogeneity is one reason to ruin model transferability (Gao *et al.* 2014a). Theoretically, additional data are helpful for us to gain a deeper understanding of hydrological processes, to improve model performance and benefit model transferability; however, which information will practically be valuable is still an open question, requires more stringent hypothesis tests and more case studies.

The forcing data spatial heterogeneity has been well documented (Barry 1992; Willmott & Matsuura 1995; Daly *et al.* 2008; Yu *et al.* 2012). Since most meteorological stations in mountainous regions are located in valleys and impacted by local relief on precipitation and energy distribution, the observed meteorological data may not be able to represent the spatial distribution pattern (Klemes 1990; Hrachowitz & Weiler 2011). Immerzeel *et al.* (2015) found that the observed precipitation severely underestimates the actual precipitation in the upper Indus basin, which was essential to estimate the water balance. Regarding its impact on model performance, most studies have shown that involving distributed forcing data has improved model performance (Boyle *et al.* 2001; Andréassian *et al.* 2004; Ajami *et al.* 2006) and consistency (Euser *et al.* 2015), with the exception of Kling & Gupta (2009), who found that spatial distributed input is of less importance than physical properties. However, how the spatial distribution of forcing data impacts on snow and ice melting simulation and model transferability is still unclear.

Concerning the impact of topography on snow and ice melt, the physical process has been intensively studied (Luce *et al.* 1998; Jost *et al.* 2007; Ménard *et al.* 2014), and well coupled into hydrological models (Bloschl *et al.* 1991; Seibert 1997; Pomeroy *et al.* 2007). However, few studies have investigated the impact of topography on snow/ice hydrologic model performance to simulate hydrography and transferability. Therefore, whether considering topography merely increases model complexity or truly improves model performance and its transferability still needs to be investigated.

Snow and ice melt in cold and mountainous catchments in Central Asia (Immerzeel & Bierkens 2012; Li *et al.* 2016) plays an essential role to support the economic sustainable development in the middle stream, and maintain the health of ecosystems in the downstream surrounded by deserts (Shi *et al.* 2000; Yao *et al.* 2007; Qin & Ding 2010; Cheng *et al.* 2014). For example, snow and ice melt accounts for half of surface runoff for the entire Urumqi River basin (Ma 1999). In Tarim River, a neighbor catchment of the Urumqi River basin, glacier melt accounts for over 40% of

the total surface runoff (Liu *et al.* 2006). The snow and ice cover are monitored both by field survey and remote sensing, and a large amount of data has been collected (Liu *et al.* 2014). However, how to use this information to aid hydrological modeling and whether this type of information will improve model performance are still unaddressed questions.

In this study, we tested the hypothesis that adding forcing data spatial distribution, topography, and snow and ice information will improve model performance and transferability in a glacier catchment in Central Asia. Compared with other auxiliary information, i.e., groundwater storage and fluctuation, saturated area fraction, or isotopic data, topographic information and snow and ice data are more easily observable, more reliable and with less uncertainty. Therefore, it is worthwhile to test the benefit of this type of auxiliary information to improve model performance and transferability. Particularly, we selected a well-gauged catchment – the Urumqi Glacier No.1 catchment – as a case study to conduct the research. A stepwise modeling framework was implemented. First, we used the meteorological station observed precipitation and temperature as forcing data, to test the results of model simulation and transferability. Second, we took forcing data spatial distribution into account, and did the same test. Third, the local relief, i.e., aspect, was considered. Finally, the simulation of snow and ice was incorporated as part of the objective function to do calibration and then transferability tests.

STUDY SITE AND DATA

Study site

The Urumqi No.1 Glacier catchment is located in northwest China, Central Asia. It is the headwater of Urumqi River which sustains five million residents in the downstream. The elevation ranges from 3,740 to 4,490 m a.s.l. The Glacier No.1 runoff gauge station (No.1) controls an area of 3.34 km^2, with 55% covered by ice. Another gauge station in the downstream, Zong Kong (ZK), controls an area of 28.9 km^2, with 21% covered by glaciers. The non-glacierized areas are mainly bare soil/rock with sparse grass (Li *et al.* 2010), with shallow root zone storage capacity (Gao *et al.* 2014b).

Datasets

The No.1 Glacier has the longest glaciology measurement record in China. The observation program started in 1959 (Xie & Ge 1965) and has continued up to the present day. Field observations include yearly glacier accumulation and ablation, daily meteorological and hydrological data collection.

Streamflow is observed at two runoff gauging stations, the No.1 and ZK. Daily streamflow is available during the main snow/glacier melting season (June–August) from 1985 to 2006 (Table 1). Daily meteorological data are available from the Da Xi Gou (DXG) meteorological station located at 3,539 m a.s.l., about 3 km downstream of the glacier (Figure 1) for the period 1958–2006. Between March 1987 and February 1988, Yang *et al.* (1992) conducted an intensive snow survey close to the DXG meteorological station. Daily snow depth and snow density were measured, from which the daily snow water equivalent (SWE) was derived.

The variations of glacier mass balance (GMB) and equilibrium line altitude (ELA) sensitively indicates and quantifies the glacier change with climate change (Cuffey & Paterson 2010). Both the GMB and ELA were observed by stake method, with a permanent stake network, properly distributed across different elevation zones (about 45–80 stakes in 8–9 rows) and additional snow pits (Ye *et al.* 2005). From the monthly change of stakes' height above the ice surface in hydrological years (from the beginning

Table 1 | Observed variables, the periods of observation, and the time step of data

Data	Period of observation	Time step
Streamflow in No.1	1985–1998, 2001–2004	Daily
Streamflow in ZK	1985–1995, 1997–2004	Daily
Air temperature	1959–2006	Daily
Precipitation	1959–2006	Daily
SWE	03/1987–02/1988	Daily
GMB of Glacier No.1	1959–2006, (1967–1979 reconstructed)	Annual
ELA of Glacier No.1	1959–2006, (1967–1979 reconstructed)	Annual

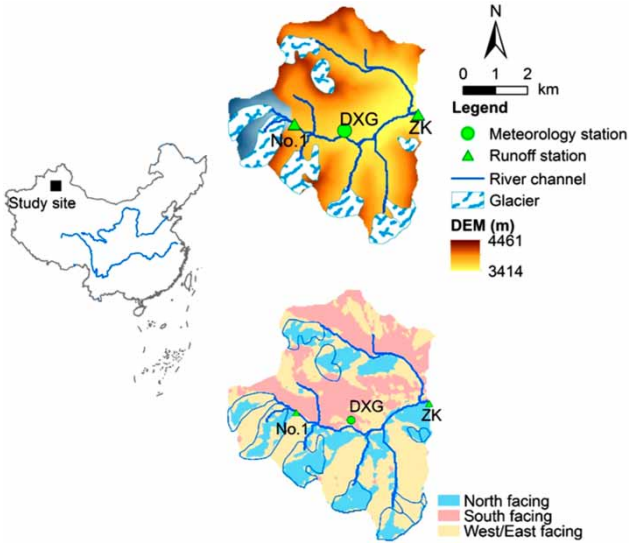

Figure 1 | Locations of the Glacier No.1 (left); the digital elevation model (DEM) and glaciers cover of the ZK catchment; and the aspects of the ZK catchment.

of October to the end of the next September), we can calculate the ice mass balance of each observation point in that year. Based on point measurement, the GMB of the entire glacier can be calculated by the contour map (Elder *et al.* 1992). The annual ELA is the altitude at where the ice accumulation and ablation are equal over a hydrological year, in other words, it is where the mass balance was zero of that year (Dong *et al.* 2012). The annual GMB and ELA are available from 1959 to 1966, and from 1980 to 2006. From 1967 to 1979, the observation was stopped, and the GMB and ELA data for the (1967–1979) period were reconstructed based on the relationship between air temperature and observed GMB (Zhang 1981).

Topography discretization

Topography influences forcing data spatial distribution and the energy budget (e.g., Barry 1992), thus also glacier and snow distribution and melting. This is particularly true for elevation and aspect, which directly impact solar radiation allocation as the first order control on snow/ice melt (Hock 2005). To account for these influences, balancing accuracy with computational cost, the catchments in this study were discretized into 16 elevation zones in the Glacier No.1 and 21 in the ZK catchment, with 50 m intervals to do elevation classification. Subsequently, each elevation zone was further divided into three aspect zones, including the north (315–45 °), south (135–225 °), and the east/west (45–135 ° and 225–315 °) facing aspects. In summary, considering elevations, aspects as well as glaciered and non-glaciered areas, the Glacier No.1 catchment was classified into 96 classes, and ZK was classified into 126 classes.

Forcing data and their interpolation

The long-term mean annual temperature is −5.1 °C, with −20 °C in winter and about 0 °C from June to August. The annual precipitation is around 450 mm a^{-1}, and snow is the main phase of precipitation in the glacier area and the non-glacier area in non-summer seasons. Over 90% of precipitation occurs between April and September. Potential evaporation was calculated by the Hamon equation (Hamon 1961) and reaches a long-term average of about 200 mm a^{-1}. In the Hamon equation, only temperature is required as input, with no any free parameters to be calibrated. Oudin *et al.* (2005) found that the performance of rainfall–runoff simulation is not very sensitive with different approaches to estimate potential evaporation, therefore we chose this parsimonious method in this study.

The DXG meteorological station is located in low elevated valleys to allow easier access for maintenance, which typically reduces the representativeness of the observed variables. To offset these biases, temperature in the individual elevation zones was corrected with a lapse rate of −0.007° m^{-1} (Li *et al.* 2013), while precipitation was adjusted with a lapse rate of 0.05% m^{-1} (Yang *et al.* 1988).

METHODS

Model

Snow model

Separate snowfall and rainfall. Precipitation is simulated to be either snow (P_s) or rain (P_l) depending on whether the daily average air temperature (T) is above or below a threshold temperature, T_t [°C] (Equations (1) and (2)) (Han *et al.* 2010). It is worthwhile to note that with more detailed

auxiliary information, a dynamic scheme can be a competent alternative to estimate the snowfall (Ding *et al.* 2014).

$$P_s = \begin{cases} P; & T \le T_t \\ 0; & T > T_t \end{cases} \quad (1)$$

$$P_l = \begin{cases} P; & T > T_t \\ 0; & T \le T_t \end{cases} \quad (2)$$

Snowfall correction. Caused by systematic errors in measurement, such as wind wetting and evaporative losses, snowfall is always being underestimated (Goodison *et al.* 1998; Yang *et al.* 2001). According to field observation in this study site, Yang *et al.* (1988) concluded that only 76.5% snowfall is captured by observation in this study site. Therefore, the amount of observed snowfall should be multiplied by 1.3 to correct the biased observation.

Snowmelt simulation. The snow pack was regarded as porous media which can hold the liquid melting/rainfall water and the liquid water could be refrozen into the snow pack. Therefore, the solid snow pack (S_w) and the liquid water inside the snow pack (S_{wl}) were conceptualized as two separate reservoirs. The water balance of the S_w reservoir is shown in Equation (3), where R_{rf} (mm d^{-1}) is the refreezing water from S_{wl} to S_w. M_s (mm d^{-1}) indicates the melted snow. Equation (4) shows the water balance of S_{wl} reservoir, where the P_e (mm d^{-1}) means the effective precipitation from snow pack to soil and the SWE is the sum of solid and liquid water of snow pack. Snowmelt (M_s) is calculated with the widely used temperature-index approach (Equation (5)) (Braithwaite & Olesen 1989; Hock 2003), which uses a degree-day factor F_{dd} (mm (°C d)$^{-1}$) to calculate melt water by the temperature above the threshold temperature T_t (°C). The liquid water in the S_{wl} from meltwater and rainfall is retained within the snowpack until it exceeds a certain fraction, C_{wh} (-), of the solid SWE (S_w) (Equation (6)) (Seibert 1997). Liquid water within the snowpack refreezes according to Equation (7). F_{rr} (-) is the correct factor to simulate liquid water refreezing, while temperature is below T_t (Seibert 1997).

$$\frac{dS_w}{dt} = P_s + R_{rf} - M_s \quad (3)$$

$$\frac{dS_{wl}}{dt} = P_l + M_s - R_{rf} - P_e \quad (4)$$

$$M_s = \begin{cases} F_{dd}(T - T_t); & T > T_t \\ 0; & T \le T_t \end{cases} \quad (5)$$

$$P_e = \begin{cases} \frac{dS_{wl}}{dt} - C_{wh}\frac{dS_w}{dt}; & S_{wl} > C_{wh}S_w \\ 0; & S_{wl} \le C_{wh}S_w \end{cases} \quad (6)$$

$$R_{rf} = \begin{cases} F_{dd}F_{rr}(T_t - T); & T_t > T \\ 0; & T_t \le T \end{cases} \quad (7)$$

Model for non-glacier area

Unsaturated reservoir. The water balance of the unsaturated reservoir (S_u) is

$$\frac{dS_u}{dt} = P_e - E_a - R_u \quad (8)$$

where P_e (mm d^{-1}) is the effective rainfall to soil; E_a (mm d^{-1}) is the actual evaporation, which was assumed to equal to potential evaporation, since energy is not the constraint factor for evaporation in this region (Kang *et al.* 2002); R_u (mm d^{-1}) is the streamflow generated from the unsaturated reservoir (Equation (8)). Water retention curve of the Xinanjiang model (Equation (9)) (Zhao 1992) was used to separate P_e into retained water in S_u and R_u, and $S_{u,max}$ (mm) is the root zone storage capacity and β (–) is the shape parameter.

$$\frac{R_u}{P_e} = 1 - \left(1 - \frac{S_u}{(1+\beta)S_{u,max}}\right)^{\beta} \quad (9)$$

Response reservoir in non-glacier area. A splitter D (–) was applied to divide the R_u into two fluxes (R_f and R_s) and into two response reservoirs (S_f and S_s). We used two linear reservoirs (S_f and S_s) to represent the response process of subsurface storm flow Q_f (mm d^{-1}) and groundwater streamflow Q_s (mm d^{-1}).

$$\frac{dS_f}{dt} = R_f - Q_f \quad (10)$$

$$\frac{dS_s}{dt} = R_s - Q_s \tag{11}$$

$$Q_f = \frac{S_f}{K_f} \tag{12}$$

$$Q_s = \frac{S_s}{K_s} \tag{13}$$

where R_f (mm d^{-1}) is the recharge into fast response reservoir (S_f); and R_s (mm d^{-1}) is the recharge into slow response reservoir (S_s); K_f (d) is the recession parameter of S_f; and K_s (d) is the recession parameter of S_s.

Glacier melting and mass balance

If the ice is covered by snow, the energy is first provided to melt snow. The ice only starts to melt without snow cover. The temperature-index method is used to simulate glacier melt M_g (mm d^{-1}) (Equation (14)). Mainly due to the lesser albedo of ice cover (Fujita & Sakai 2014), the degree-day factor of glaciers is larger than snow degree-day factor in the same region (Braithwaite & Olesen 1989; Seibert *et al.* 2014). Therefore, we use a multiplier (C_g) to get the glacier degree-day factor by F_{dd}.

$$M_g = \begin{cases} F_{dd}C_g(T - T_t); & T > T_t \ \& \ S_w = 0 \\ 0; & T \le T_t \text{ or } S_w > 0 \end{cases} \tag{14}$$

The response routine on ice is calculated by an independent linear reservoir S_g (Equations (15) and (16)), with a recession parameter K_g (d).

$$\frac{dS_g}{dt} = P_e + M_g - Q_g \tag{15}$$

$$Q_g = \frac{S_g}{K_g} \tag{16}$$

The GMB of each elevation band (S_g) can be derived from precipitation (P) on glaciers and simulated glacier streamflow (Q_g).

$$\frac{dS_g}{dt} = P - Q_g \tag{17}$$

The sum of the S_g weighted by their area proportion is the GMB of the entire glacier. It is worthwhile to note that the calculated annual GMB is the water equivalent, which should be transformed into the ice thickness before comparing with measured GMB, divided by the ice density (0.91 g/cm^3). The ELA is the altitude where accumulation and ablation are equal at a given period.

Snow/ice melting on different aspects

With the same air temperature, the south facing aspects get more direct solar radiation, which provides the most critical energy source for snow/ice melting (Hock 2005), and resulting in more melting water; while the north facing aspects get less direct solar radiation due to the topography shadow impact. The east/west facing aspects receive the intermediate solar radiation and then melting water with the same air temperature. The influence of aspect is taken into account by a multiplier C_a (–), which is larger than 1. Specifically, the F_{dd} in south facing aspects are multiplied by C_a, and the north facing aspects are multiplied by $1/C_a$, and the east/west facing aspects are kept as F_{dd}.

Model calibration and evaluation approach

Objective functions

The Kling-Gupta efficiency (Gupta *et al.* 2009) (I_{KGE}) was used as objective function for calibration and the criteria to evaluate model performance. The equation is:

$$I_{KGE} = 1 - \sqrt{(r-1)^2 + (\alpha - 1)^2 + (\beta - 1)^2} \tag{18}$$

where r is the linear correlation coefficient between simulation and observation; α ($\alpha = \sigma_m/\sigma_o$) is a measure of relative variability in the simulated and observed values, where σ_m is the standard deviation of simulated streamflow, and σ_o is the standard deviation of observed streamflow; β is

the ratio between the average value of simulated and observed data.

Model evaluation

Some parameters are obtained from observation or the literature, such as the temperature lapse rate (Li *et al.* 2013), the precipitation lapse rate (Yang *et al.* 1988), and the snowfall correction factor (Yang *et al.* 1988) (Table 2).

Additionally, there are 13 free parameters to be calibrated. In order to calibrate the model and analyze the model uncertainty, the generalized likelihood uncertainty estimation (GLUE) (Beven & Binley 1992) was applied. The I_{KGE} is set as the objective function. The prior ranges of parameters are mostly determined by the literature, and are shown in Table 2. Monte Carlo was applied to sample 50,000 sets of parameters within prior ranges, and then the best 1% (500 parameter sets) was selected as behavioral parameter sets to do further analysis. The daily streamflow from 1985 to 1996 was used to do calibration, while the rest of daily streamflow data were severed to validate the models. All the models were warmed-up by one year spin-up period.

Experiments

We designed four model setups to conduct four virtual experiments. Forcing data, model structure, and method to calculate the objective function were modified step by step.

Experiment 1 ($M_{nA}F_PO_H$)

Develop a glacier hydrological model, whose detailed information was described in the section 'Model'. The impact of elevation on forcing data distribution and the influence of aspect on melting are not taken into account in this experimental scenario. The *in situ* observed meteorological data were used as input. Measured hydrograph was utilized to calibrate parameters and evaluate model performance with I_{KGE} of hydrograph as the objective function. We named this model setup '$M_{nA}F_PO_H$', indicating the model not accounting for aspect, forcing by point meteorological observation, and using only the hydrograph simulation as the objective function. Subsequently, test the model transferability by transferring both model and behavioral parameter sets from No.1 catchment to ZK catchment.

Table 2 | Model parameters and their prior ranges for Monte Carlo sampling in GLUE method

Parameters	Description	Unit	Prior range	Method to estimate
L_t	Temperature lapse rate	$^{\circ}Cm^{-1}$	0.007	Li *et al.* (2013)
L_p	Precipitation lapse rate	$\%m^{-1}$	0.05	Yang *et al.* (1988)
C_s	Snowfall correction factor	–	1.3	Yang *et al.* (1988)
T_t	Threshold temperature to split snowfall and rainfall	$^{\circ}C$	(0, 4)	Han *et al.* (2010)
F_{dd}	Degree-day factor of snow	mm $(^{\circ}C\ d)^{-1}$	(2, 9)	Zhang *et al.* (2006); Yang *et al.* (2012)
C_g	Factor for ice melt	–	(1, 2)	Gao *et al.* (2012)
C_a	Factor for the influence of aspect on melt	–	(1, 2)	Gao *et al.* (2012)
C_{wh}	Snow water holding capacity	–	(0, 1)	Gao *et al.* (2012)
F_{rr}	Refreezing factor	–	(0, 1)	Gao *et al.* (2012)
$K_{f,g}$	Recession coefficient of glacier streamflow	D	(1, 10)	Gao *et al.* (2014a)
$S_{u,max}$	Root zone storage capacity	mm	(30, 100)	Gao *et al.* (2012, 2014b)
β	Shape parameter	–	(0.1, 1)	Gao *et al.* (2012)
D	The splitter	–	(0.2, 0.8)	Gao *et al.* (2014a)
K_f	Recession coefficient of fast response reservoir	d	(2, 30)	Gao *et al.* (2014a)
K_s	Recession coefficient of slow response reservoir	d	(30, 200)	Gao *et al.* (2014a)

Experiment 2 ($M_{nA}F_DO_H$)

Keep model structure and objective function the same as $M_{nA}F_PO_H$ while changing the input forcing data from *in situ* observed data to the spatial distributed forcing data, considering the lapse rates of precipitation and temperature. Calibrate and validate the glacier hydrological model, and then test its capability to be transferred. We named this model setup '$M_{nA}F_DO_H$', indicating the model does not account for aspect, forced by distributed precipitation and temperature, and using hydrograph simulation as the objective function.

Experiment 3 ($M_AF_DO_H$)

In this virtual experiment, the impact of aspect on snow/ice melting was taken into account with the approach described in the section 'Snow/ice melting on different aspects'. The spatial distributed forcing data and the calibration approach are kept the same as $M_{nA}F_DO_H$, while the effect of different proportions of aspects at distinct elevation bands was considered in the Glacier No.1 catchment while doing calibration and validation, and the ZK catchment in the model transferability test. This experimental setup was named '$M_AF_DO_H$', indicating the model accounts for aspect, forced by distributed observation data, and using hydrograph simulation as the objective function.

Experiment 4 ($M_AF_DO_{HGS}$)

Snow and ice accumulation and ablation is an essential sub-routine in this landscape-based hydrological model. Using the model structure and distributed forcing proposed in Experiment 3, we attempted to further test if cooperating the snow and ice auxiliary information in calibration could improve model performance on reproducing hydrograph and snow/ice, and the ability to be transferred and upscaled. Technically, we utilized not only the hydrograph simulation as the objective function to evaluate the model performance, but also took the snow and ice sub-routine simulation into account, by quantifying the simulation of SWE, GMB, and ELA into the objective function. The objective function (I_{KGE_HGS}) was applied to evaluate model performance of hydrograph and the snow/ice sub-routine simulation, by giving different weights to hydrograph (I_{KGE_H}), SWE (I_{KGE_SWE}), GMB (I_{KGE_GMB}), and ELA (I_{KGE_ELA}) (Equation (19)). This new objective function allows us to restrict the behavioral parameters' distribution by involving snow and ice information in calibration. Then, test whether the model transferability will be improved by this auxiliary information. This experimental setup was named '$M_AF_DO_{HGS}$'.

$$I_{KGE\_HGS} = 0.7I_{KGE\_H} + 0.1I_{KGE\_SWE} + 0.1I_{KGE\_GMB} + 0.1I_{KGE\_ELA} \quad (19)$$

RESULTS AND DISCUSSION

Models' calibration and temporal validation

The summary of four model setups ($M_{nA}F_PO_H$, $M_{nA}F_DO_H$, $M_AF_DO_H$, and $M_AF_DO_{HGS}$) in calibration and validation are shown in Figure 2. The results show that the first three model setups ($M_{nA}F_PO_H$, $M_{nA}F_DO_H$, and $M_AF_DO_H$) can reproduce hydrographs quite well in calibration, all the median values of I_{KGE} are above 0.7, with the highest I_{KGE} values around 0.8. Compared with the benchmark model setup ($M_{nA}F_PO_H$), there is no obvious improvement in calibration when involving spatial distribution of forcing data ($M_{nA}F_DO_H$). Taking into account the aspect information has slightly improved model calibration when comparing $M_AF_DO_H$ with $M_{nA}F_DO_H$. It is not a surprise that the $M_AF_DO_{HGS}$ does not perform well in calibration, compared with the other three model setups, although its median value of the I_{KGE} is above 0.7 as well. Since accounting for snow and ice simulation in the objective function will filter out the parameters fitting both hydrograph and snow and ice simultaneously, it may reduce the model performance if hydrograph is the only evaluation criterion. This is in line with other research on multi-objective calibration (Fenicia *et al.* 2007). In summary, all models can be used to fit the observed hydrographs by calibration, even neglecting the impacts of forcing data distribution and topography.

Furthermore, Figure 2 demonstrates that the four model setups all perform satisfactorily in temporal validation, with

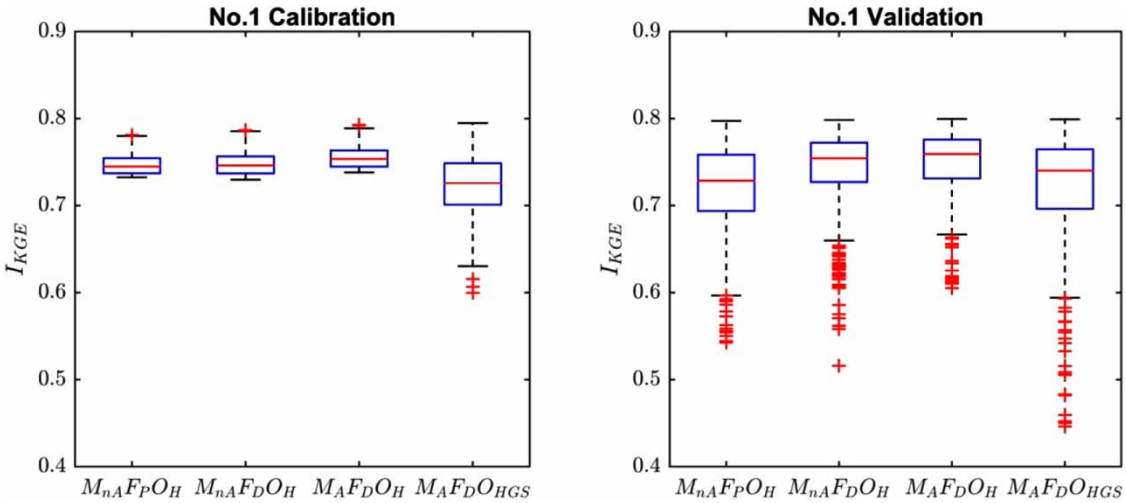

Figure 2 | Calibration and validation results the four model setups in Glacier No.1 catchment. The lines in the boxes indicate the medians, boxes of the 25/75th, and whiskers the 5/95th quantiles.

median values of I_{KGE} above 0.7. Not surprisingly, both the boxes of the 25/75th quantiles and whiskers of the 5/95th quantiles for all model setups have wider ranges compared with the calibrated results. Additionally, there are more outliers below 5% quantiles, indicating the validation results have larger uncertainty than for calibration. While comparing the four model setups in validation, both forcing data spatial distribution and the impact of aspect on snow/ice melting have improved model validation. This means these two pieces of auxiliary information can increase model simulation consistence (Euser *et al.* 2015). Interestingly, the median value of $M_AF_DO_{HGS}$ in validation is even better than its performance in calibration. It is probably caused by the better data quality in 1995–2005 than the calibration period (1985–1994).

Figure 3 shows the comparison between observed and calibrated hydrographs of the four model setups in the Glacier No.1 catchment, in 1986. The simulated hydrographs do not exhibit distinctive differences among these four model setups in calibration. In all these four setups, no matter if point or distributed forcing input, regardless of whether taking account of the aspect, or whether involving snow and ice into the objective function, all model setups can well reproduce the hydrographs. This means all of them have the ability to fit hydrograph by calibration. Interestingly, the hydrograph components (glacier and non-glacier runoff) simulated by the four model setups are also surprisingly comparable. This illustrates that the most part of the streamflow is contributed from the glacier area, and further confirms the reliability and robustness of hydrograph components' simulation. Noticeably, both the observed and simulated hydrographs show similar variation with temperature, but are distinct regarding the fluctuation of rainfall. This illustrates the sensitivity of glacier melt and hydrograph with temperature change in this highly glaciered catchment. Quantitatively, with one unit area, the glacier area generates four to five times more streamflow than the non-glacier area.

Parameters' uncertainty

Figure 4 shows the dotty plot of the parameters of the four model setups and their averaged values, generated by the GLUE parameter uncertainty estimation method. It is worthwhile noting that the parameters related to snow and ice accumulation and ablation are well identified in all the four model setups, which is in line with other research (van den Broeke *et al.* 2010; Hegdahl *et al.* 2016). Particularly well identifiable are the parameter controlling rainfall/snowfall split threshold temperature (T_t), degree-day factor (F_{dd}), glacier melt multiply factor (C_g), hold capacity of snow pack (C_{wh}), recession parameter of glacier zone ($K_{f,g}$). This provides further evidence supporting the fact that the hydrological process in this catchment is mostly influenced by snow and glacier melt. Less identifiability of the correct

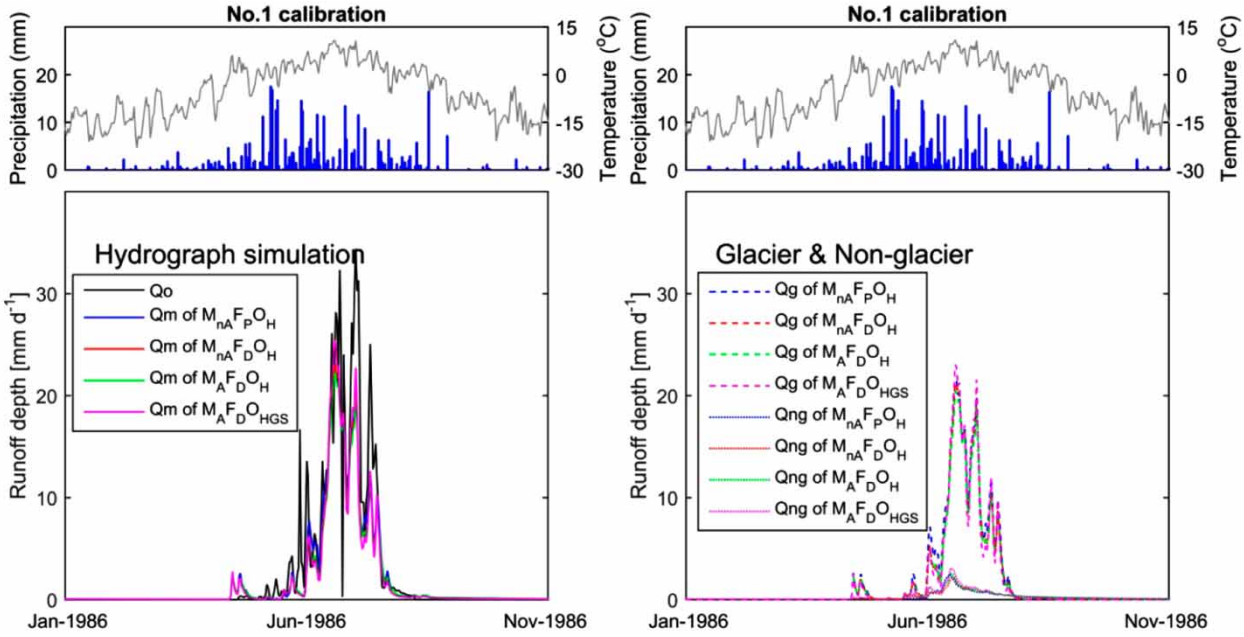

Figure 3 | The observed daily average air temperature and daily precipitation; and the comparison between observed and the modelled daily streamflow. The right figure shows the streamflow generated by four model setups of glacier and non-glacier area in the Glacier No.1 catchment.

factor to simulate liquid water refreezing in snow cover F_{rr} (-) may indicate the lesser importance of the refreezing process in the melting season in this study site, due to the relative thin snow cover (Qin *et al.* 2006) compared with a humid area (Pulliainen 2006). The aspect multiple factor (C_a) for $M_AF_DO_H$ and $M_AF_DO_{HGS}$ is also not as identifiable as other snow- and ice-related parameters, which probably indicates the aspect information, to some extent, has been implicitly considered in the glacier distribution data due to the influence of aspect on spatial distribution of glaciers (Figure 1). Simultaneously, the parameters intended to simulate the non-glacierized areas, are not well identifiable, such as $S_{u,max}$, β, C_e, K_f, K_s. Therefore, the signal of non-glacier hydrograph components are harder to identify from hydrograph.

In Figure 5, the cumulative distribution of behavioral parameters is illustrated. If the accumulative values are close to diagonal, this indicates the behavioral parameters are close to uniform distribution. The farther the accumulative distribution to the diagonal is, the better identifiability of the parameter is. We can find that glacier- and snow-related parameters are distributed farther to the diagonal, indicating their better identifiability, while the non-glacier-related parameters have the opposite pattern. It is worthwhile to note that the distribution of parameter D in $M_AF_DO_{HGS}$ is different from its distribution pattern in other model setups. This parameter is a splitter to separate the generated runoff into the fast and slow response reservoirs. Larger D value indicates more water will go to the fast response reservoir, and less water to the slow one. Therefore, different D values will impact the shape of the hydrograph. Since $M_AF_DO_{HGS}$ involves both hydrograph and snow/ice simulation to estimate the objective function, the trade-off between hydrograph and snow/ice simulation may impact on the distribution of this parameter. This trade-off may cause the parameters controlling the shape of hydrographs to be not well represented.

Remarkably, both Figures 4 and 5 illustrate that the $M_{nA}F_PO_H$ model setup has the most identifiable parameter sets for snow and ice accumulation and melt. However, its simulation consistence indicated by validation is not as good as other model scenarios. If we use the parameter identifiability to judge the model uncertainty, we may draw the conclusion that $M_{nA}F_PO_H$ model setup performs better with less uncertainty compared with other model setups, which is obviously not true. This result shows the parameter distribution is not a good indicator to judge the model performance or realism. We can only safely address that if the parameters are well

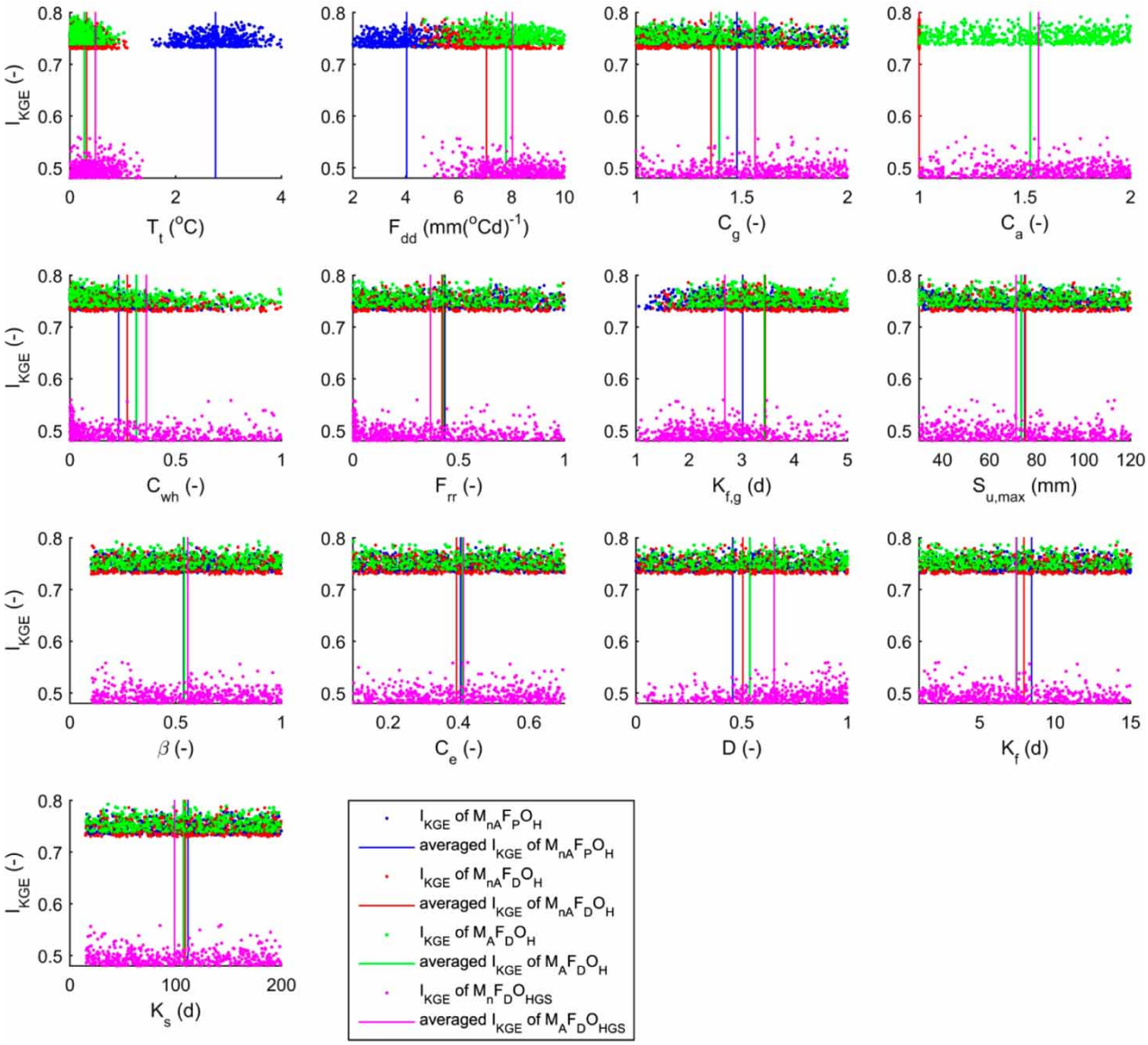

Figure 4 | Parameter dotty plots of four model setups. The lines indicate the averaged value of the behavioral parameters.

identified, which indicates the importance of certain hydrological processes represented by the parameters. There is no direct linkage between model reliability, model performance, and the parameter identifiability.

Moreover, we can also find the trade-off between related parameters, such as T_t and F_{dd}. For example, the $M_{nA}F_PO_H$ fits hydrography with larger T_t than the other model setups, which indicates snowfall occurs and starts to melt with higher temperature. On the one hand, this increases the proportion of snowfall, and simultaneously decreases the positive degree-days for snow and ice melting, therefore larger degree-day factor (F_{dd}) is needed to compensate the change. This parameter's trade-off phenomenon might be hidden in calibration by compensation, but could be amplified if we do model validation and parameter transfer.

Snow and ice simulation

The observed and simulated SWE from March 1st, 1987 to February 29th, 1988 are shown in Figure 6. Interestingly,

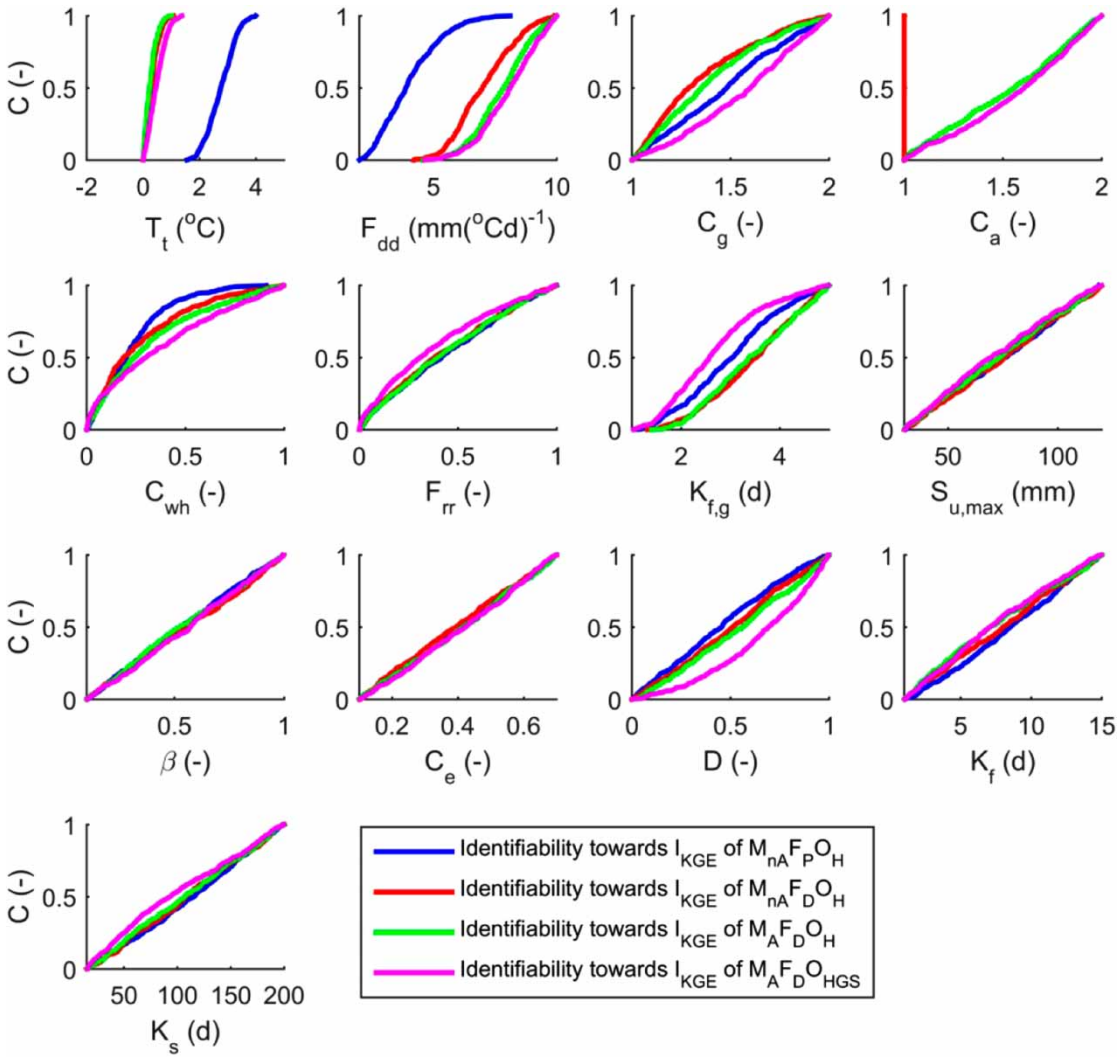

Figure 5 | Identifiability of model parameters toward the related objectives. The performance measures based on which the cumulative performance C (-) is calculated are determined from the values of I_{KGE}.

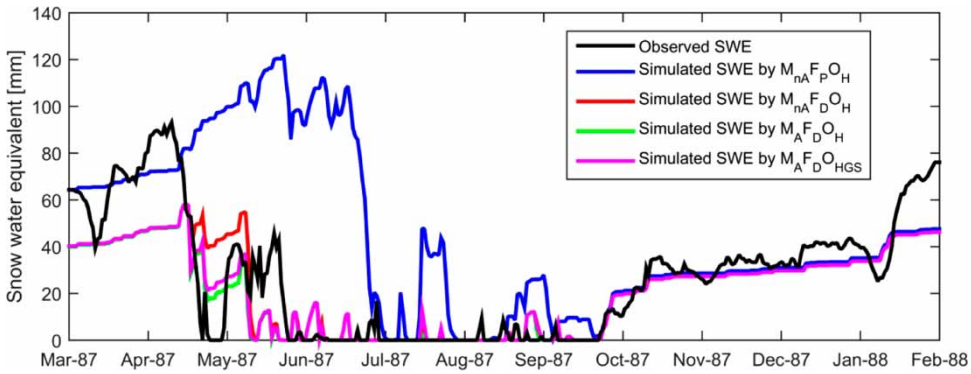

Figure 6 | Comparison between the observed and the modelled daily snow water equivalent (SWE) from March 1987 to February 1988.

all four model setups perform well from October 1987 to February 1988. This indicates the limited uncertainty in this period, but from March 1987 to September 1987, the four models perform quite distinctively. The simulated SWE by $M_{nA}F_PO_H$ is quite different from observation and other simulation, with large overestimation of the snow pack. From the parameter distribution in Figures 4 and 5, we can find $M_{nA}F_PO_H$ has larger T_t than other model setups. This means that with higher threshold temperature for snowfall, the $M_{nA}F_PO_H$ is prone to calculate more snowfall than other scenarios with the same temperature data. This overestimation is caused by neglecting the spatial distribution of forcing data. This result also illustrates that a model can reproduce hydrograph excellently, but it does not guarantee that it will satisfy the internal fluxes inspection. Once the forcing data distribution was taken into account, $M_{nA}F_DO_H$ improves the snow pack simulation conspicuously. Comparing with $M_AF_DO_H$ and $M_AF_DO_{HGS}$, $M_{nA}F_DO_H$ starts to melt almost simultaneously but with less amount, which is caused by the comparable T_t value but smaller degree-day factor. The simulated SWEs by $M_AF_DO_H$ and $M_AF_DO_{HGS}$ are quite similar. It is almost impossible to separate these two lines apart in most time series. This supports the model structure, algorithm, and forcing data of $M_AF_DO_H$, allowing the outstanding simulation of SWE even without involving snow information in calibration.

The observed and simulated (by three model setups, $M_{nA}F_DO_H$, $M_AF_DO_H$, and $M_AF_DO_{HGS}$) GMB and ELA are exhibited in Figure 7. Given the ignorance of elevation bands in the $M_{nA}F_DO_H$ model setup, it is impossible to calculate the ELA, and the estimated GMB without elevation bands does not make sense either. Therefore, the simulated GMB and ELA were not demonstrated. Figure 7 shows the comparable fluctuation pattern of simulated GMB and ELA of three model setups. The simulated GMB and ELA by three model setups are very close, which is especially true for $M_AF_DO_H$ and $M_AF_DO_{HGS}$. Remarkably, the results support that with the same model structure and algorithm to simulate the snow and ice ablation and melting, merely adding the auxiliary information of snow and ice while calculating objective function is not beneficial to improve model performance in this case study, even only for the inspection of snow and ice sub-routine.

Model transferability

Figure 8 shows the performance of the four model setups in transferability test from Glacier No.1 catchment to ZK catchment. $M_{nA}F_PO_H$ is the last option for model transferability, with the lowest median value, and the widest range of the 25/75th quantiles boxes and 5/95th quantiles whiskers which indicate the largest uncertainty. Figure 9 shows the simulated hydrographs and hydrograph components from glacier and non-glacier areas of four model setups in the ZK catchment, while transferring both the model setup and the behavioral parameters from the donor catchment (Glacier No.1). The result obtained by $M_{nA}F_PO_H$ performs worst among these four model setups. Especially in the beginning of the melting season, $M_{nA}F_PO_H$ underestimates the amount of streamflow, and the estimated start time to melt was later than observation. When melting starts, snow melt first begins from lower elevations of the catchment, but the lumped forcing data did not consider this heterogeneity. Melting starts only when the lumped temperature is above the threshold temperature (T_t), which is later than the real start time and does not fit the physical realism.

Impact of forcing data distribution

The improvement of the median values of I_{KGE} while involving forcing data distribution ($M_{nA}F_DO_H$) is exhibited in Figure 8. The 25/75th quantiles boxes and 5/95th quantiles whiskers also become narrower, demonstrating the declining of uncertainty. The results support the hypotheses that involving the forcing data distribution will increase the model realism to reproduce catchment hydrological processes. The simulated hydrograph (Figure 9) by $M_{nA}F_DO_H$ is also closer to the observed one, both in the perspective of the amount of streamflow and the start time of melting. The hydrograph components in Figure 9 show that the peak flow generated from the glacier area in the $M_{nA}F_DO_H$ is larger than the $M_{nA}F_PO_H$, while the streamflow from the non-glacier area in the $M_{nA}F_DO_H$ is smaller than the $M_{nA}F_PO_H$. Different from $M_{nA}F_PO_H$, in which glacier and non-glacier areas almost simultaneously contribute to streamflow, non-glacier areas melt earlier than glacier areas in $M_{nA}F_DO_H$ due to the lower elevation of non-glacier areas.

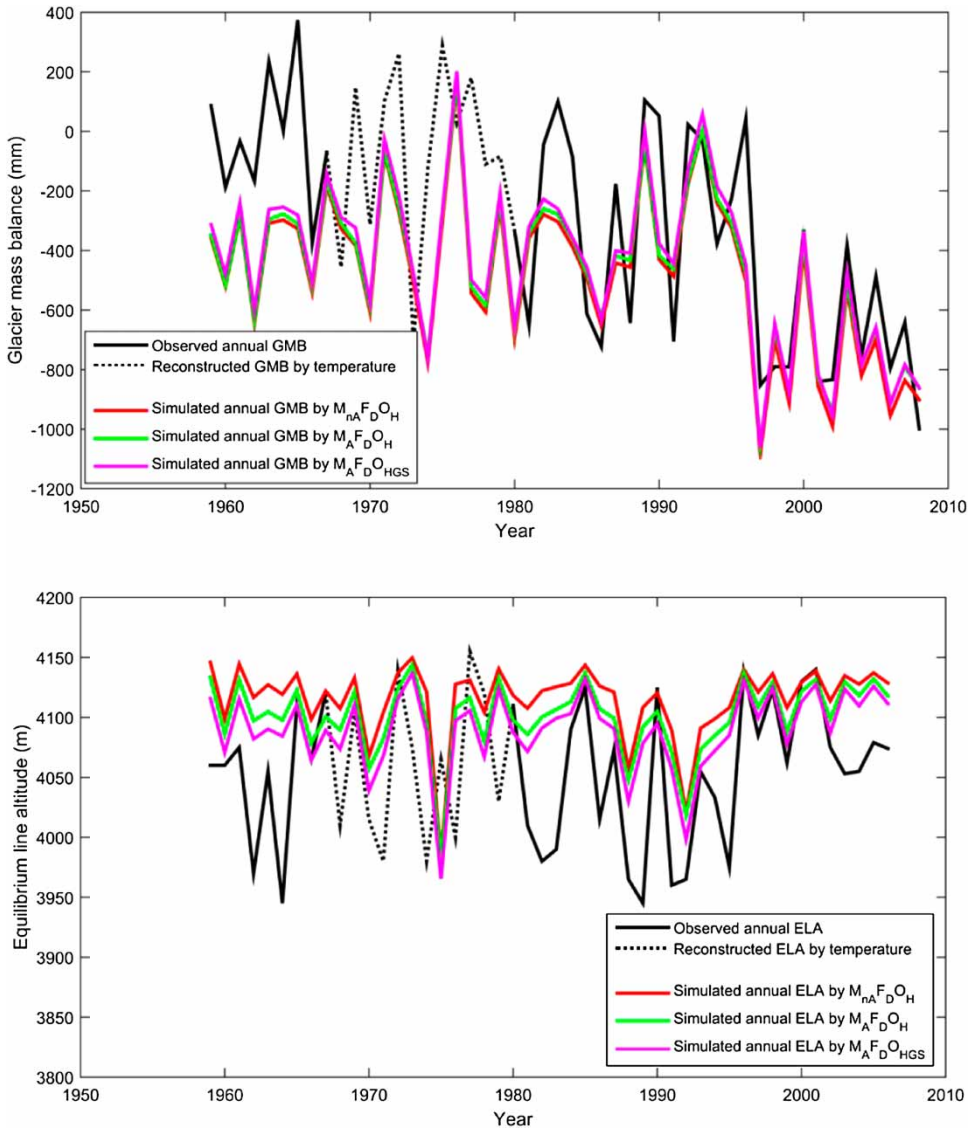

Figure 7 | Upper panel shows the observed and modelled (by $M_{nA}F_DO_H$, $M_AF_DO_H$, and $M_AF_DO_{HGS}$ model setups) glacier mass balance (GMB) of the Urumqi No.1 Glacier from 1959 to 2008. Lower panel shows modelled and observed equilibrium line altitude (ELA) of the Urumqi No.1 Glacier from 1958 to 2006. Dashed lines represent the GMB and ELA reconstructed by temperature data from 1967 to 1979.

Impact of aspect

Model transferability is also beneficial by considering the impact of aspect on melting ($M_AF_DO_H$) (Figure 8). The simulated hydrograph by $M_AF_DO_H$ in model transfer is closer to the observed one compared with $M_{nA}F_DO_H$ and the other two model setups ($M_{nA}F_PO_H$ and $M_AF_DO_{HGS}$), with less uncertainty and higher median value. Figure 9 shows the improved hydrograph simulation by $M_AF_DO_H$ when involving aspect as auxiliary information, although not as significantly as taking account of the spatial distributed forcing data.

Given that glacier melt is the dominant hydrological process in these two catchments, it is worthwhile to analyze the glacier distribution for different aspects to understand the influence of aspect on model transferability. By map algebra, we analyzed the aspect map together with the glacier map, and found that 55% of the Glacier No.1 catchment is covered by glacier: 52% is covered by east/west facing glacier, 46% with north facing glacier, and less

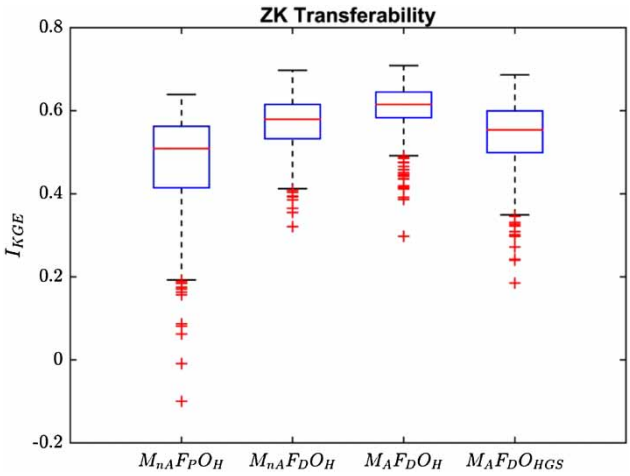

Figure 8 | Model transferability results of four model scenarios.

than 2% covered with south facing ice. While in the ZK catchment, 21% is covered by glaciers: 43% is covered by east/west facing glacier, 55% is covered by north facing glacier, and 2% is covered by south facing ice. The results interestingly showed the clear pattern of glacier distribution. In both catchments, east/west and north facing aspects shared around 50% of the glaciers, and the area of south facing glaciers is limited. This may be caused by the fact that the location of glacier is strongly impacted by aspect, due to the spatial distribution pattern of solar radiation caused by topography, and eventually the snow and ice accumulation and melt. The transferability test illustrates that since the aspect information is implicitly contained in the glacier distribution pattern, further involving aspect could improve model transferability, but not as remarkably as considering the impact of elevation on forcing data.

Impact of snow and ice information

The first three model scenarios ($M_{nA}F_PO_H$, $M_{nA}F_DO_H$, and $M_AF_DO_H$) only employ hydrograph to do calibration validation and transferability test. While $M_AF_DO_{HGS}$ involved snow and ice simulation as part of the objective function for calibration. The snow and ice auxiliary information, used to constrain the model parameters, includes GMB and ELA of glaciers, and SWE of snow pack. Figures 8 and 9 show that after adding the snow and ice auxiliary information in calibration, there is no improvement of model transferability. This indicates involving the auxiliary information does not guarantee the improvement of model performance in well-gauged catchment.

The reason is probably caused by the fact that the dominant hydrological processes have been fairly reflected in the observed hydrograph and the well-designed model. Moreover, the key processes of submodels have been

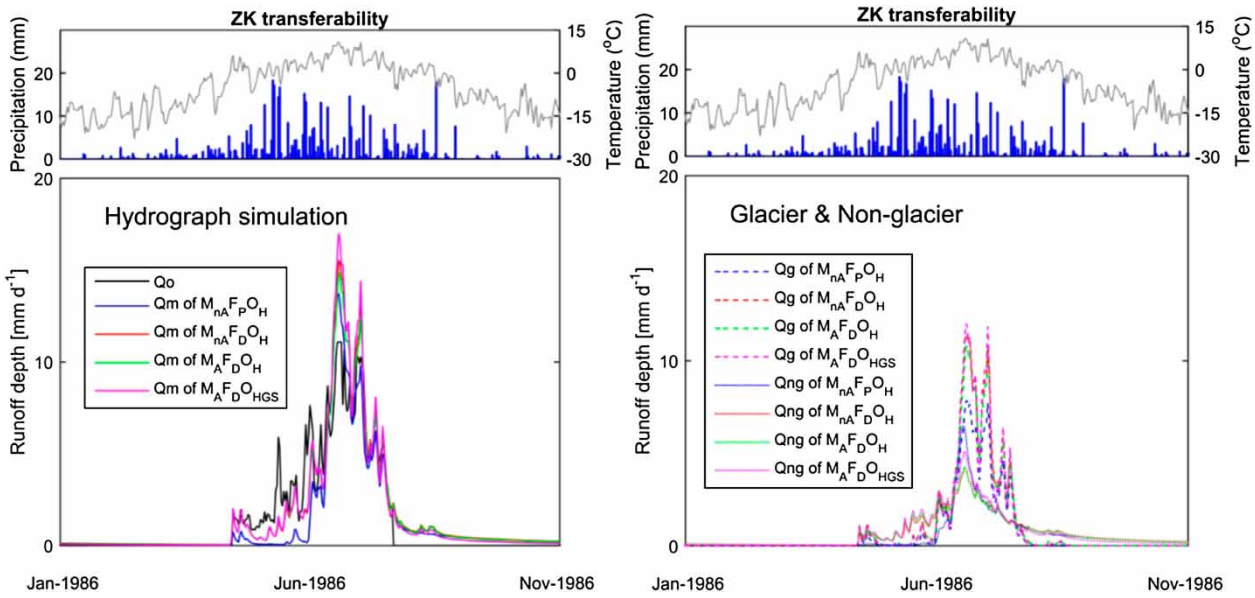

Figure 9 | Observed daily average air temperature and daily precipitation; and the comparison between observed and the modelled daily streamflow. The right figure shows the streamflow generated by four model scenarios of glacierized and non-glacierized area in the ZK catchment.

well-constrained by hydrograph while doing parameter calibration. Precisely, Figures 6 and 7 show that snow and ice accumulation and ablation processes have been well represented in the $M_AF_DO_H$ model even though there is no snow and ice information applied to constrain the parameter calibration. Another interpretation might be the data quality of auxiliary information. In many cases, the auxiliary information is more difficult to access than conventional data. Due to the difficulty of doing measurements, the data quality of auxiliary information is probably not as reliable as hydrograph observation in well-gauged runoff stations. Moreover, the $M_AF_DO_H$ model setup has taken catchment heterogeneity into account properly, including the elevation zones, aspects, and landscape classification (glacier/non-glacierized areas), which probably makes the auxiliary snow and ice data redundant.

This study also guides us to improve model transferability by more reliable spatial distributed forcing data and more realistic model structure. Besides, in some cases, auxiliary information will not guarantee the improvement of model realism and model transferability. Moreover, involving the snow and ice information in objective functions may lead the calibration to put extra effort into snow and ice simulation, which weakens the impact of hydrograph simulation in objective functions and causes deterioration in the performance of calibration and validation in the criteria of I_{KGE}. This may also result in the slight deterioration of model transferability.

It is not uncommon that hydrological models, especially the landscape-based models, have been criticized by equifinality (Beven & Binley 1992), mainly caused by more complicated model structure and larger amount of parameters, compared with lumped models. However, this study shows that with more realistic model structure, the equifinality can be well restricted, even with more complex model structure and larger amounts of parameters.

CONCLUSIONS

This study tested the impact of auxiliary information, i.e., forcing data spatial distribution, topography, and snow and ice data, on model performance and transferability. We started from a model setup ($M_{nA}F_PO_H$) without this auxiliary information. Subsequently, involving forcing data spatial distribution and the impact of aspect on snow and ice melt step by step, $M_{nA}F_DO_H$ and $M_AF_DO_H$ were developed to test the impact of these two pieces of information. The results indicate that the forcing data spatial distribution and taking account of topography to calculate snow/ice melting had a marginal effect on model calibration, but improved model validation and, more importantly, the model transferability. Interestingly, when we add snow and ice information in the objective function to do calibration, the model performance in validation and transferability is not improved; on the contrary, it slightly deteriorates model performance for streamflow simulation in this study site. The results demonstrate that cooperating auxiliary information will not guarantee a better model performance. From this study, we can draw the following conclusions:

1. Forcing data spatial distribution, including precipitation and temperature, is essential in a snow and ice melt dominant catchment, and helpful to improve model performance in validation and model transferability.
2. Accounting for topography, i.e., aspect, in glacier and snow melting model can increase model realism and improve model transferability, but not as obvious as the forcing data spatial distribution, because the aspect information, to some extent, has been implicitly involved while coupling the glacier distribution information.
3. Well-gauged hydro-meteorological data might be sufficient to constrain a well-designed hydrological model. Involving the snow and ice data to constrain model parameters does not guarantee the improvement of model performance for streamflow simulation and model transferability.

ACKNOWLEDGEMENTS

This research is supported by State Key Laboratory of Cryospheric Sciences, Cold and Arid Regions Environment and Engineering Research Institute, Chinese Academy Sciences (SKLCS-OP-2016-04), and National Natural Science Foundation of China (41471001). We thank two anonymous reviewers for their constructive comments and valuable suggestion which dramatically

improved the quality of this paper. Thanks also go to Fabrizio Fenicia for his review and corrections of the draft manuscript.

REFERENCES

Ajami, N. K., Duan, Q., Gao, X. & Sorooshian, S. 2006 Multimodel combination techniques for analysis of hydrological simulations: application to distributed model intercomparison project results. *Journal of Hydrometeorology* **7** (4), 755–768. DOI:10.1175/JHM519.1.

Andréassian, V., Oddos, A., Michel, C., Anctil, F., Perrin, C. & Loumagne, C. 2004 Impact of spatial aggregation of inputs and parameters on the efficiency of rainfall-runoff models: a theoretical study using chimera watersheds. *Water Resources Research* **40** (5). DOI:10.1029/2003WR002854.

Baldocchi, D., Falge, E., Gu, L., Olson, R., Hollinger, D., Running, S., Anthoni, P., Bernhofer, C., Davis, K., Evans, R., Fuentes, J., Goldstein, A., Katul, G., Law, B., Lee, X., Malhi, Y., Meyers, T., Munger, W., Oechel, W. K. T., Paw, U., Pilegaard, K., Schmid, H. P., Valentini, R., Verma, S., Vesala, T., Wilson, K. & Wofsyn, S. 2001 FLUXNET: A new tool to study the temporal and spatial variability of ecosystem–scale carbon dioxide, water vapor, and energy flux densities. *Bulletin of the American Meteorological Society* **82** (11), 2415–2434. DOI:10.1175/1520-0477(2001)082 < 2415:FANTTS > 2.3.CO;2.

Barry, R. G. 1992 *Mountain Weather and Climate.* Cambridge University Press, USA.

Beven, K. & Binley, A. 1992 The future of distributed models: model calibration and uncertainty prediction. *Hydrological Processes* **6**, 279–298. DOI:10.1002/hyp.3360060305.

Beven, K. J. & Kirkby, M. J. 1979 A physically based, variable contributing area model of basin hydrology. *Hydrological Sciences Bulletin* **24** (1), 43–69. DOI:10.1080/02626667909491834.

Biondi, D. & De Luca, D. L. 2017 Rainfall-runoff model parameter conditioning on regional hydrological signatures: application to ungauged basins in southern Italy. *Hydrology Research* **48** (3), 714–725. DOI:10.2166/nh.2016.097.

Bloschl, G., Kirnbauer, R. & Gutknecht, D. 1991 Distributed snowmelt simulations in an alpine catchment I. Model evaluation on the basis of snow cover patterns. *Water Resources Research* **27** (12), 3171–3179. DOI:10.1029/91WR02250.

Boyle, D. P., Gupta, H. V., Sorooshian, S., Koren, V., Zhang, Z. & Smith, M. 2001 Toward improved streamflow forecasts: value of semidistributed modeling. *Water Resources Research* **37** (11), 2749–2759. DOI:10.1029/2000WR000207.

Braithwaite, R. J. & Olesen, O. B. 1989 *Calculation of Glacier Ablation from Air Temperature, West Greenland.* Springer, Dordrecht, The Netherlands.

Cheng, G., Li, X., Zhao, W., Xu, Z., Feng, Q., Xiao, S. & Xiao, H. 2014 Integrated study of the water–ecosystem–economy in the Heihe River basin. *National Science Review*. DOI:10.1093/nsr/nwu017.

Cuffey, K. M. & Paterson, W. S. B. 2010 *The Physics of Glaciers.* Academic Press, Cambridge, MA.

Daly, C., Halbleib, M., Smith, J. I., Gibson, W. P., Doggett, M. K., Taylor, G. H., Curtis, J. & Pasteris, P. P. 2008 Physiographically sensitive mapping of climatological temperature and precipitation across the conterminous United States. *International Journal of Climatology* **28** (15), 2031–2064. DOI:10.1002/joc.1688.

Ding, B., Yang, K., Qin, J., Wang, L., Chen, Y. & He, X. 2014 The dependence of precipitation types on surface elevation and meteorological conditions and its parameterization. *Journal of Hydrology* **513**, 154–163. DOI:10.1016/j.jhydrol.2014.03.038.

Dong, Z., Qin, D., Ren, J., Li, K. & Li, Z. 2012 Variations in the equilibrium line altitude of Urumqi Glacier No. 1, Tianshan Mountains, over the past 50 years. *Chinese Science Bulletin* **57** (36), 4776–4783.

Duan, Z. & Bastiaanssen, W. G. M. 2013 Estimating water volume variations in lakes and reservoirs from four operational satellite altimetry databases and satellite imagery data. *Remote Sensing of Environment* **134**, 403–416. DOI:10.1016/j.rse.2013.03.010.

Elder, K., Kattelmann, R., Ushnurtsev, S., Yang, D. & Chichagov, A. 1992 Differences in mass balance calculations resulting from alternative measurement and estimation techniques on Glacier No. 1, Tien Shan, China. *Annals of Glaciology* **16**, 198–206.

Euser, T., Hrachowitz, M., Winsemius, H. C. & Savenije, H. H. G. 2015 The effect of forcing and landscape distribution on performance and consistency of model structures. *Hydrological Processes* **29** (17), 3727–3743. DOI:10.1002/hyp.10445.

Fenicia, F., Savenije, H. H. G., Matgen, P. & Pfister, L. 2007 A comparison of alternative multiobjective calibration strategies for hydrological modeling. *Water Resources Research* **43** (3). DOI:10.1029/2006WR005098.

Fenicia, F., McDonnell, J. J. & Savenije, H. H. G. 2008 Learning from model improvement: on the contribution of complementary data to process understanding. *Water Resources Research* **44** (6). DOI:10.1029/2007WR006386.

Fujita, K. & Sakai, A. 2014 Modelling runoff from a Himalayan debris-covered glacier. *Hydrology and Earth System Sciences* **18** (7), 2679–2694. DOI:10.5194/hess-18-2679-2014.

Gao, H., He, X., Ye, B. & Pu, J. 2012 Modeling the runoff and glacier mass balance in a small watershed on the Central Tibetan Plateau, China, from 1955 to 2008. *Hydrological Processes* **26** (11), 1593–1603. DOI:10.1002/hyp.8256.

Gao, H., Hrachowitz, M., Fenicia, F., Gharari, S. & Savenije, H. H. G. 2014a Testing the realism of a topography-driven model (FLEX-Topo) in the nested catchments of the Upper Heihe, China. *Hydrology and Earth System Sciences* **18** (5), 1895–1915. DOI:10.5194/hess-18-1895-2014.

Gao, H., Hrachowitz, M., Schymanski, S. J., Fenicia, F., Sriwongsitanon, N. & Savenije, H. H. G. 2014b Climate controls how ecosystems size the root zone storage capacity at catchment scale. *Geophysical Research Letters* **41** (22), 7916–7923. DOI:10.1002/2014GL061668.

Gharari, S., Hrachowitz, M., Fenicia, F. & Savenije, H. H. G. 2011 Hydrological landscape classification: investigating the performance of HAND based landscape classifications in a central European meso-scale catchment. *Hydrology and Earth System Sciences* **15** (11), 3275–3291. DOI:10.5194/hess-15-3275-2011.

Goodison, B. E., Louie, P. Y. T. & Yang, D. 1998 *WMO Solid Precipitation Measurement Intercomparison*. World Meteorological Organization, Instruments and Observing Methods Report No. 67.

Gupta, H. V., Kling, H., Yilmaz, K. K. & Martinez, G. F. 2009 Decomposition of the mean squared error and NSE performance criteria: implications for improving hydrological modelling. *Journal of Hydrology* **377** (1–2), 80–91. DOI:10.1016/j.jhydrol.2009.08.003.

Hailegeorgis, T. T. & Alfredsen, K. 2015 Comparative evaluation of performances of different conceptualisations of distributed HBV runoff response routines for prediction of hourly streamflow in boreal mountainous catchments. *Hydrology Research* **46** (4), 607–628.

Hamon, W. R. 1961 Estimating potential evapotranspiration. *Journal of the Hydraulics Division* **87** (3), 107–120.

Han, C., Chen, R. S., Liu, J., Yang, Y. & Qing, W. 2010 A discussion of separating solid and liquid precipitation. *Journal of Glaciology and Geocryology* **32**, 249–256.

Hegdahl, T. J., Tallaksen, L. M., Engeland, K., Burkhart, J. F. & Xu, C.-Y. 2016 Discharge sensitivity to snowmelt parameterization: a case study for Upper Beas basin in Himachal Pradesh, India. *Hydrology Research* **47** (4), 683–700. DOI: 10.2166/nh.2016.047.

Hock, R. 2003 Temperature index melt modelling in mountain areas. *Journal of Hydrology* **282** (1–4), 104–115. DOI:10.1016/S0022-1694(03)00257-9.

Hock, R. 2005 Glacier melt: a review of processes and their modelling. *Progress in Physical Geography* **29** (3), 362–391. DOI:10.1191/0309133305pp453ra.

Hrachowitz, M. & Weiler, M. 2011 Uncertainty of precipitation estimates caused by sparse gauging networks in a small, mountainous watershed. *Journal of Hydrologic Engineering* **16** (5), 460–471. DOI:10.1061/(ASCE)HE.1943-5584.0000331.

Hrachowitz, M., Savenije, H. H. G., Blöschl, G., McDonnell, J. J., Sivapalan, M., Pomeroy, J. W., Arheimer, B., Blume, T., Clark, M. P., Ehret, U., Fenicia, F., Freer, J. E., Gelfann, A., Gupta, H. V., Hughes, D. A., Hut, R. W., Montanari, A., Pande, S., Tetzlaff, D., Troch, P. A., Uhlenbrook, S., Wagener, T., Winsemius, H. C., Woods, R. A., Zehe, E. & Cudennec, C. 2013 A decade of predictions in ungauged basins (PUB) – a review. *Hydrological Sciences Journal* **58** (6), 1198–1255. DOI:10.1080/02626667.2013.803183.

Immerzeel, W. W. & Bierkens, M. F. P. 2012 Asia's water balance. *Nature Geoscience* **5** (12), 841–842. DOI:10.1038/ngeo1643.

Immerzeel, W. W., Wanders, N., Lutz, A. F., Shea, J. M. & Bierkens, M. F. P. 2015 Reconciling high-altitude precipitation in the upper Indus basin with glacier mass balances and runoff. *Hydrology and Earth Systems Science Journal* **19** (11), 4673–4687. DOI:10.5194/hess-19-4673-2015.

Jost, G., Weiler, M., Gluns, D. R. & Alila, Y. 2007 The influence of forest and topography on snow accumulation and melt at the watershed-scale. *Journal of Hydrology* **347** (1–2), 101–115. DOI: http://dx.doi.org/10.1016/j.jhydrol.2007.09.006.

Kang, E. S., Cheng, G. D., Lan, Y. C., Chen, R. S. & Zhang, J. S. 2002 Application of a conceptual hydrological model in the runoff forecast of a mountainous watershed. *Advance in Earth Sciences* **17** (1), 18–26.

Kirchner, J. W. 2006 Getting the right answers for the right reasons: linking measurements, analyses, and models to advance the science of hydrology. *Water Resources Research* **42** (3). DOI:10.1029/2005WR004362.

Klaus, J. & McDonnell, J. J. 2013 Hydrograph separation using stable isotopes: review and evaluation. *Journal of Hydrology* **505**, 47–64. DOI:10.1016/j.jhydrol.2013.09.006.

Klemes, V. 1990 The modelling of mountain hydrology: the ultimate challenge. *Hydrology Mountainous Areas*. IAHS Publication No. 190, 29–43.

Kling, H. & Gupta, H. 2009 On the development of regionalization relationships for lumped watershed models: the impact of ignoring sub-basin scale variability. *Journal of Hydrology* **373** (3–4), 337–351. DOI:10.1016/j.jhydrol.2009.04.031.

Li, Z., Wang, W., Zhang, M., Wang, F. & Li, H. 2010 Observed changes in streamflow at the headwaters of the Urumqi River, eastern Tianshan, central Asia. *Hydrological Processes* **24** (2), 217–224. DOI:10.1002/hyp.7431.

Li, X., Wang, L., Chen, D., Yang, K., Xue, B. & Sun, L. 2013 Near-surface air temperature lapse rates in the mainland China during 1962–2011. *Journal of Geophysical Research: Atmospheres* **118** (14), 7505–7515. DOI:10.1002/jgrd.50553.

Li, H., Xu, C.-Y. & Beldring, S. 2015a How much can we gain with increasing model complexity with the same model concepts? *Journal of Hydrology* **527**, 858–871. DOI: http://dx.doi.org/10.1016/j.jhydrol.2015.05.044.

Li, H., Beldring, S., Xu, C.-Y., Huss, M. & Melvold, K. 2015b Integrating a glacier retreat model into a hydrological model – case studies on three glacierised catchments in Norway and Himalayan region. *Journal of Hydrology* **527**, 656–667. doi:10.1016/j.jhydrol.2015.05.017.

Li, H., Xu, C.-Y., Beldring, S., Tallaksen, T. M. & Jain, S. K. 2016 Water resources under climate change in Himalayan basins. *Water Resources Management* **30**, 843–859. DOI:10.1007/s11269-015-1194-5.

Lindström, G. 2016 Lake water levels for calibration of the S-HYPE model. *Hydrology Research* **47** (4), 672–682. DOI: 10.2166/nh.2016.019.

Liu, S., Ding, Y., Shangguan, D., Zhang, Y., Li, J., Han, H., Wang, J. & Xie, C. 2006 Glacier retreat as a result of climate warming and increased precipitation in the Tarim river basin, northwest China. *Annals of Glaciology* **43** (1), 91–96.

Liu, S., Shangguan, D., Xu, J., Wang, X., Yao, X., Jiang, Z., Guo, W., Lu, A., Zhang, S., Ye, B., Li, Z., Wei, J. & Wu, L. 2014 Glacier in China and their variations. In: *Global Land Ice Measurements from Space* (J. S. Kargel, G. J. Leonard, M. P. Bishop, A. Kääb & B. H. Raup, eds). Springer, Heidelberg, Germany, pp. 583–608.

Luce, C. H., Tarboton, D. G. & Cooley, K. R. 1998 The influence of the spatial distribution of snow on basin-averaged snowmelt. *Hydrological Processes* **12** (10–11), 1671–1683. DOI:10.1002/(SICI)1099-1085(199808/09)12:10/11 < 1671::AID-HYP688 > 3.0.CO;2-N.

Ma, X. 1999 *Flood and Drought Hazards of Inland River in Northwest China.* Yellow River Hydraulic Press, Zhengzhou, China.

Matgen, P., Fenicia, F., Heitz, S., Plaza, D., de Keyser, R., Pauwels, V. R. N., Wagner, W. & Savenije, H. 2012 Can ASCAT-derived soil wetness indices reduce predictive uncertainty in well-gauged areas? A comparison with in situ observed soil moisture in an assimilation application. *Advances in Water Resources* **44**, 49–65. DOI: http://dx.doi.org/10.1016/j.advwatres.2012.03.022.

Ménard, C. B., Essery, R. & Pomeroy, J. 2014 Modelled sensitivity of the snow regime to topography, shrub fraction and shrub height. *Hydrology and Earth System Sciences Journal* **18** (6), 2375–2392. DOI:10.5194/hess-18-2375-2014.

Moore, R. D., Fleming, S. W., Menounos, B., Wheate, R., Fountain, A., Stahl, K., Holm, K. & Jakob, M. 2009 Glacier change in western North America: influences on hydrology, geomorphic hazards and water quality. *Hydrological Processes* **23** (1), 42–61. DOI:10.1002/hyp.7162.

Oudin, L., Michel, C. & Anctil, F. 2005 Which potential evapotranspiration input for a lumped rainfall-runoff model? Part 1 – Can rainfall-runoff models effectively handle detailed potential evapotranspiration inputs? *Journal of Hydrology* **303** (1–4), 275–289. DOI:10.1016/j.jhydrol.2004.08.025.

Pomeroy, J. W., Gray, D. M., Brown, T., Hedstrom, N. R., Quinton, W. L., Granger, R. J. & Carey, S. K. 2007 The cold regions hydrological model: a platform for basing process representation and model structure on physical evidence. *Hydrological Processes* **21** (19), 2650–2667. DOI:10.1002/hyp.6787.

Pulliainen, J. 2006 Mapping of snow water equivalent and snow depth in boreal and sub-arctic zones by assimilating space-borne microwave radiometer data and ground-based observations. *Remote Sensing of Environment* **101** (2), 257–269. DOI: http://dx.doi.org/10.1016/j.rse.2006.01.002.

Qin, D. & Ding, Y. 2010 Key issues on cryospheric changes, trends and their impacts. *Advances in Climate Change Research* **1**, 1–10.

Qin, D., Liu, S. & Li, P. 2006 Snow cover distribution, variability, and response to climate change in Western China. *Journal of Climate* **19** (9), 1820–1833. DOI:10.1175/JCLI3694.1.

Refsgaard, J. C., Madsen, H., Andréassian, V., Arnbjerg-Nielsen, K., Davidson, T. A., Drews, M., Hamilton, D. P., Jeppesen, E., Kjellström, E., Olesen, J. E., Sonnenborg, T. O., Trolle, D., Willems, P. & Christensen, J. H. 2014 A framework for testing the ability of models to project climate change and its impacts. *Climatic Change* **122** (1–2), 271–282. DOI:10.1007/s10584-013-0990-2.

Seibert, J. 1997 Estimation of parameter uncertainty in the HBV model. *Hydrology Research* **28** (4–5), 247–262.

Seibert, J. 2003 Groundwater dynamics along a hillslope: a test of the steady state hypothesis. *Water Resources Research* **39** (1), 1–9. DOI:10.1029/2002WR001404.

Seibert, J., Jenicek, M., Huss, M. & Ewen, T. 2014 Snow and ice in the hydrosphere. In: *Snow and Ice-Related Hazards, Risks, and Disasters* (W. Haeberli, C. Whiteman & J. F. Schroder, eds). Elsevier, Amsterdam, p. 99.

Shi, Y., Huang, M. & Yao, T. 2000 *Glaciers and Their Environments in China – The Present, Past and Future.* Science Press, Beijing.

Singh, P., Haritashya, U. K. & Kumar, N. 2008 Modelling and estimation of different components of streamflow for Gangotri Glacier basin, Himalayas. *Hydrological Sciences Journal* **53** (2), 309–322. DOI:10.1623/hysj.53.2.309.

Sun, J., Li, Y. P., Huang, G. H. & Wang, C. X. 2017 Analysis of interactive effects of DEM resolution and basin subdivision level on runoff simulation in Kaidu River Basin, China. *Hydrology Research* **48** (4), 1100–1117. DOI:10.2166/nh.2016.332.

Tangdamrongsub, N., Steele-Dunne, S. C., Gunter, B. C., Ditmar, P. G. & Weerts, A. H. 2015 Data assimilation of GRACE terrestrial water storage estimates into a regional hydrological model of the Rhine River basin. *Hydrology and Earth System Sciences Journal* **19** (4), 2079–2100. DOI:10.5194/hess-19-2079-2015.

Troch, F. P., Verhoest, N., Gineste, P., Paniconi, C. & Mérot, P. 2001 Variable source areas, soil moisture and active microwave observations at Zwalmbeek and Coët-Dan. In: *Spatial Patterns in Catchment Hydrology: Observations and Modelling* (R. Grayson & G. Bloschl, eds). Cambridge University Press, Cambridge, UK, pp. 187–208.

Uhlenbrook, S. & Hoeg, S. 2003 Quantifying uncertainties in tracer-based hydrograph separations: a case study for two-, three- and five-component hydrograph separations in a mountainous catchment. *Hydrological Processes* **17** (2), 431–453. DOI:10.1002/hyp.1134.

van den Broeke, M., Bus, C., Ettema, J. & Smeets, P. 2010 Temperature thresholds for degree-day modelling of Greenland ice sheet melt rates. *Geophysical Research Letters* **37** (18). DOI:10.1029/2010GL044123.

Weiler, M., McGlynn, B. L., McGuire, K. J. & McDonnell, J. J. 2003 How does rainfall become runoff? A combined tracer and runoff transfer function approach. *Water Resources Research* **39** (11). DOI:10.1029/2003WR002331.

Willmott, C. J. & Matsuura, K. 1995 Smart interpolation of annually averaged air temperature in the United States. *Journal of Applied Meteorology* **34** (12), 2577–2586. DOI:10.1175/1520-0450(1995)034 < 2577:SIOAAA > 2.0.CO;2.

Winsemius, H. C., Savenije, H. H. G., van de Giesen, N. C., van den Hurk, B. J. J. M., Zapreeva, E. A. & Klees, R. 2006 Assessment of gravity recovery and climate experiment (GRACE) temporal signature over the upper Zambezi. *Water Resources Research* **42** (12). DOI:10.1029/2006WR005192.

Winsemius, H. C., Schaefli, B., Montanari, A. & Savenije, H. H. G. 2009 On the calibration of hydrological models in ungauged basins: a framework for integrating hard and soft hydrological information. *Water Resources Research* **45** (12), W12422. DOI:10.1029/2009wr007706.

Xiao, J., Chen, J., Davis, K. J. & Reichstein, M. 2012 Advances in upscaling of eddy covariance measurements of carbon and water fluxes. *Journal of Geophysical Research: Biogeosciences* **117** (G1). DOI:10.1029/2011JG001889.

Xie, Z. & Ge, G. 1965 Study of accumulation, ablation and mass balance of glacier no. 1 at the headwater of Urumqi river, Tianshan. In: *Study of Glaciology and Hydrology on the Urumqi River, Tianshan* (Lanzhou Institute of Glaciology and Geocryology, Chinese Academy of Sciences). Science Press, Beijing, pp. 14–24.

Yang, D., Goodison, B., Metcalfe, J., Louie, P., Elomaa, E., Hanson, C., Golubev, V., Gunther, T., Milkovic, J. & Lapin, M. 2001 Compatibility evaluation of national precipitation gage measurements. *Journal of Geophysical Research* **106** (D2), 1481. DOI:10.1029/2000JD900612.

Yang, D., Jiang, T., Zhang, Y. & Ersi, K. 1988 Analysis and correction of errors in precipitation measurement at the head of Urumqi River, Tianshan. *Journal of Glaciology and Geocryology* **4**, 1.

Yang, D., Zhang, Y. & Zhang, Z. 1992 A study on the snow density in the head area of Urumqi River basin. *Acta Geographica Sinica* **47**, 260–266.

Yang, M., Ye, B., Peng, P., Han, T., Gao, H., Cui, Y., Wang, J. & Gao, M. 2012 A simulation of glacier runoff at headwaters of the Urumqi River. *Journal of Glaciology and Geocryology* **34**, 130–138.

Yao, T., Pu, J., Lu, A., Wang, Y. & Yu, W. 2007 Recent glacial retreat and its impact on hydrological processes on the Tibetan Plateau, China, and surrounding regions. *Arctic, Antarctic, and Alpine Research* **39**, 642–650. DOI:10.1657/1523-0430(07-510)[yao]2.0.co;2.

Ye, B., Yang, D., Jiao, K., Han, T., Jin, Z., Yang, H. & Li, Z. 2005 The Urumqi River source Glacier No. 1, Tianshan, China: changes over the past 45 years. *Geophysical Research Letters* **32** (21), L21504. DOI:10.1029/2005GL024178.

Yu, Z., Lu, Q., Zhu, J., Yang, C., Ju, Q., Yang, T., Chen, X. & Sudicky, E. 2012 Spatial and temporal scale effect in simulating hydrologic processes in a watershed. *Journal of Hydrologic Engineering* **19** (1), 99–107. DOI:10.1061/(ASCE)HE.1943-5584.0000762.

Zhang, J. 1981 Mass balance studies on glacier no. 1 in Urumqi river, Tianshan. Journal of Glaciology and Geocryology **3**, 32–40.

Zhang, Y., Liu, S. & Ding, Y. 2006 Observed degree-day factors and their spatial variation on glacier in western China. *Annals of Glaciology* **41**, 301–306.

Zhao, R.-J. 1992 The Xinanjiang model applied in China. *Journal of Hydrology* **135** (1–4), 371–381. DOI:10.1016/0022-1694(92)90096-E.

First received 9 May 2016; accepted in revised form 11 September 2016. Available online 2 December 2016